Pergamon

Int. J. Solids Structures Vol. 33, No. 7, pp. 1005–1021, 1996

0020–7683/96 $15.00 + .00

0020-7683(95)00081-X

ELASTODYNAMIC GREEN'S FUNCTIONS FOR A SMOOTHLY HETEROGENEOUS HALF-SPACE

B. B. GUZINA and R. Y. S. PAK
Department of Civil, Environmental and Architectural Engineering, University of Colorado, Boulder, CO 80309-0428, U.S.A.

(*Received* 22 *September* 1994; *in revised form* 23 *March* 1995)

Abstract—In this paper, the response of a vertically heterogeneous elastic half-space with a smooth modulus variation under a set of time-harmonic ring- and point-sources is derived analytically. A method of evaluation via asymptotic decomposition for the singular Green's functions is presented. In the technique, the Green's functions are decomposed into an analytical part and a residual component. Capturing the corresponding singular behavior, the analytical parts of the ring- and point-load Green's functions are expressible in terms of the elliptic integrals and algebraic functions, respectively. The residual integrals which are regular can be evaluated by numerical contour integration. To obtain correct results, one must note and take into account the existence of multiple poles along the formal path of the inversion integrals, the details of which are discussed in the paper. To highlight the various aspects of the physical problem, a set of illustrative numerical results is included.

1. INTRODUCTION

Solutions to elastodynamic boundary value problems associated with a smoothly heterogeneous semi-infinite solid are of practical significance in the field of geomechanics, seismology, and earthquake engineering because of the common occurrence of such site conditions with respect to depth as a result of the natural deposition process as well as gravity-induced stress conditions (Hardin and Drnevich, 1972). They are also relevant to the stress analysis of modern micro-electronic components whose material property may vary continuously by design. While a boundary element formulation can provide an efficient and rigorous treatment of such elastodynamic problems (Brebbia *et al.*, 1984; Pak and Ji, 1994), its full potential for engineering application involving a heterogeneous medium has thus far been limited to cases which can be simulated by homogeneous or piecewise homogeneous media (Apsel, 1979; Pak, 1987; Banerjee and Mamoon, 1990) owing to a lack of other Green's functions. As a cause of its complex mathematical description, the phenomenon of wave propagation in a smoothly heterogeneous solid is, among other aspects, generally characterized by continuous refractions which lead to curvilinear rays of travel. While the gradual modulus variation can be approximated by a multi-layered system, the resulting model can only predict piecewise-straight rays and may further suffer from various artificial inter-layer dynamic phenomena which are not present in the true physical problem.

In this paper, a set of fundamental Green's functions for a vertically heterogeneous half-space with a linear shear wave velocity profile is presented. Through the use of a method of potentials, it is shown that the influence fields for internal ring- and point-loads can be expressed as a combination of a number of Bessel integrals. To facilitate their application in a computational boundary element setting, an accurate and efficient numerical procedure for the evaluation of these singular solutions is also described. Useful as benchmarks for the development and assessment of related approximate solutions, some typical results for the exact Green's functions are also provided.

2. MATHEMATICAL SOLUTION FOR A HETEROGENEOUS HALF-SPACE UNDER A GENERAL BURIED SOURCE

Of interest here is the development of a set of fundamental solutions for a vertically heterogeneous elastic half-space with a constant mass density ρ and a linear shear wave velocity profile. An example of such a problem is the case of a solid medium with Lame' constants

$$\lambda(z) = \mu(z) = \mu_0(1+bz)^2, \quad z \geqslant 0, \quad b > 0, \tag{1}$$

whose equations of motion can be written as

$$(\lambda+2\mu)\nabla(\nabla\cdot\mathbf{u}) - \mu\nabla\times\nabla\times\mathbf{u} + (\nabla\cdot\mathbf{u})\nabla\lambda + (\nabla\mathbf{u}+\nabla\mathbf{u}^{\mathrm{T}})\nabla\mu + \mathbf{f} = \rho\ddot{\mathbf{u}}. \tag{2}$$

By virtue of the displacement-potential representation

$$\mathbf{u} = \mu\nabla\left(\frac{1}{\mu}\varphi\right) + \frac{1}{\mu}\nabla\times(\mu\chi\mathbf{e}_z + \mu\nabla\times\eta\mathbf{e}_z), \tag{3}$$

in cylindrical coordinates (r, θ, z) with $\mathbf{e}_z$ being the unit vector in the z-direction, the solution to (1) and (2) can be determined in terms of the pseudo-dilatational potential φ and the pseudo-distortional potentials χ and η, which can uncouple the Navier equations (Pak and Guzina, 1995). For a time harmonic, arbitrarily-distributed buried source across the plane $z = s$ in the vertically heterogeneous half-space with

$$\tau_{zr}(r,\theta,s^-,t) - \tau_{zr}(r,\theta,s^+,t) = \{\Sigma_{m=-\infty}^{\infty} P_m(r)\,\mathrm{e}^{\mathrm{i}m\theta}\,\mathrm{e}^{\mathrm{i}\omega t}\} \tag{4}$$

$$\tau_{z\theta}(r,\theta,s^-,t) - \tau_{z\theta}(r,\theta,s^+,t) = \{\Sigma_{m=-\infty}^{\infty} Q_m(r)\,\mathrm{e}^{\mathrm{i}m\theta}\,\mathrm{e}^{\mathrm{i}\omega t}\} \tag{5}$$

$$\tau_{zz}(r,\theta,s^-,t) - \tau_{zz}(r,\theta,s^+,t) = \{\Sigma_{m=-\infty}^{\infty} R_m(r)\,\mathrm{e}^{\mathrm{i}m\theta}\,\mathrm{e}^{\mathrm{i}\omega t}\}, \tag{6}$$

where $\tau_{zr}, \tau_{z\theta}, \ldots$ are the components of the Cauchy stress tensor, it can be shown by means of Fourier decomposition and Hankel transforms that the displacement response admits the following representation:

$$u_r(r,\theta,z,t) = \Sigma_{m=-\infty}^{\infty} \int_0^{\infty} \tilde{u}_{r_m}^m(\xi,z)\xi J_m(r\xi)\,\mathrm{d}\xi\,\mathrm{e}^{\mathrm{i}m\theta}\,\mathrm{e}^{\mathrm{i}\omega t} \tag{7}$$

$$u_\theta(r,\theta,z,t) = \Sigma_{m=-\infty}^{\infty} \int_0^{\infty} \tilde{u}_{\theta_m}^m(\xi,z)\xi J_m(r\xi)\,\mathrm{d}\xi\,\mathrm{e}^{\mathrm{i}m\theta}\,\mathrm{e}^{\mathrm{i}\omega t} \tag{8}$$

$$u_z(r,\theta,z,t) = \Sigma_{m=-\infty}^{\infty} \int_0^{\infty} \tilde{u}_{z_m}^m(\xi,z)\xi J_m(r\xi)\,\mathrm{d}\xi\,\mathrm{e}^{\mathrm{i}m\theta}\,\mathrm{e}^{\mathrm{i}\omega t}. \tag{9}$$

In the above, ω is the frequency of the time-harmonic motion, $\tilde{u}_i^m$ denotes the m^{th}-order Hankel transform

$$\tilde{u}_i^m(\xi) = \int_0^{\infty} u_i(r) r J_m(r\xi)\,\mathrm{d}r, \tag{10}$$

and J_m is the Bessel function of the 1st kind of order m. Together with the displacement continuity requirement at $z = s$, the free-surface condition at $z = 0$ and the regularity condition at infinity, (4)–(6) yield

$$\tilde{u}_{zr}^{m} = \Omega_1(\xi, z; s; b)\frac{X_m - Y_m}{2\mu_0} + \Omega_2(\xi, z; s; b)\frac{Z_m}{\mu_0}, \tag{11}$$

$$\tilde{u}_{rr}^{m-1} - \mathrm{i}\tilde{u}_{\theta\theta}^{m-1} = \gamma_1(\xi, z; s; b)\frac{X_m - Y_m}{2\mu_0} + \gamma_2(\xi, z; s; b)\frac{X_m + Y_m}{2\mu_0} + \gamma_3(\xi, z; s; b)\frac{Z_m}{\mu_0}, \tag{12}$$

$$\tilde{u}_{rr}^{m+1} + \mathrm{i}\tilde{u}_{\theta\theta}^{m+1} = -\gamma_1(\xi, z; s; b)\frac{X_m - Y_m}{2\mu_0} + \gamma_2(\xi, z; s; b)\frac{X_m + Y_m}{2\mu_0} - \gamma_3(\xi, z; s; b)\frac{Z_m}{\mu_0}, \tag{13}$$

where Ω_1, Ω_2, γ_1, γ_2 and γ_3 are functions given in Appendix A involving modified Bessel functions, and X_m, Y_m and Z_m are defined by the loading in the form of

$$X_m(\xi) = \tilde{P}_m^{m-1}(\xi) - \mathrm{i}\tilde{Q}_m^{m-1}(\xi) \tag{14}$$

$$Y_m(\xi) = \tilde{P}_m^{m-1}(\xi) + \mathrm{i}\tilde{Q}_m^{m-1}(\xi) \tag{15}$$

$$Z_m(\xi) = \tilde{R}_m^{m}(\xi). \tag{16}$$

As will be illustrated in the next section, many practical fundamental solutions of interest to integral equation methods can be derived by appropriate specification of the distributed loading.

3. DYNAMIC GREEN'S FUNCTIONS FOR A HETEROGENEOUS HALF-SPACE

3.1. *Axisymmetric radial ring-load of radius* a *at* $z = s$

With the time factor $e^{i\omega t}$ suppressed henceforth for brevity, a time-harmonic radial ring-load of unit intensity acting at a depth s can be expressed as

$$\tau_{zr}(r, \theta, s^+) - \tau_{zr}(r, \theta, s^-) = \delta(r - a), \tag{17}$$

where $\delta(r)$ is the one-dimensional Dirac delta function. In the context of (4), (17) is equivalent to the case where

$$P_0(r; s) = \delta(r - a). \tag{18}$$

with $P_m = 0$ for $m \neq 0$ and $Q_m = R_m = 0$ for all m. As a result, one may write the displacement Green's functions as

$$\hat{u}_{rr}^{\mathrm{ring}}(r, \theta, z; a, s) = \frac{a}{\mu_0}\int_0^{\infty} \gamma_1(\xi, z; s; b)\xi J_1(a\xi)J_1(r\xi)\,\mathrm{d}\xi \tag{19}$$

$$\hat{u}_{r\theta}^{\mathrm{ring}}(r, \theta, z; a, s) = 0 \tag{20}$$

$$\hat{u}_{rz}^{\mathrm{ring}}(r, \theta, z; a, s) = -\frac{a}{\mu_0}\int_0^{\infty} \Omega_1(\xi, z; s; b)\xi J_1(a\xi)J_0(r\xi)\,\mathrm{d}\xi, \tag{21}$$

where the first and the second subscript denote the direction of the load and the displacement component, respectively.

3.2. *Axisymmetric torsional ring-load of radius* a *at* z = s

For the case of an axisymmetric internal torsional ring load which can be defined by

$$\tau_{z\theta}(r,\theta,s^-) - \tau_{z\theta}(r,\theta,s^+) = \delta(r-a), \tag{22}$$

its Fourier components in (4) (6) are

$$Q_0(r;s) = \delta(r-a), \tag{23}$$

$Q_m = 0$ for $m \neq 0$ and $P_m = R_m = 0$ for all m. In this case, the corresponding radial, angular and vertical components of the influence field can be expressed as

$$\hat{u}_{rr}^{\mathrm{ring}}(r,\theta,z;a,s) = 0 \tag{24}$$

$$\hat{u}_{r\theta}^{\mathrm{ring}}(r,\theta,z;a,s) = \frac{a}{\mu_0}\int_0^\infty \gamma_2(\xi,z;s;b)\xi J_1(a\xi)J_1(r\xi)\,\mathrm{d}\xi \tag{25}$$

$$\hat{u}_{rz}^{\mathrm{ring}}(r,\theta,z;a,s) = 0. \tag{26}$$

3.3. *Axisymmetric vertical ring-load of radius* a *at* z = s

A vertical ring-load of unit intensity acting in the interior of a half-space can be defined by

$$\tau_{zz}(r,\theta,s^-) - \tau_{zz}(r,\theta,s^+) = \delta(r-a), \tag{27}$$

which implies

$$R_0(r;s) = \delta(r-a), \tag{28}$$

with $R_m = 0$ for $m \neq 0$ and $P_m = Q_m = 0$ for all m. By virtue of (7) and (9), the components of the displacement influence field can be written as

$$\hat{u}_r^{\mathrm{ring}}(r,\theta,z;a,s) = -\frac{a}{\mu_0}\int_0^\infty \gamma_3(\xi,z;s;b)\xi J_0(a\xi)J_1(r\xi)\,\mathrm{d}\xi \tag{29}$$

$$\hat{u}_\theta^{\mathrm{ring}}(r,\theta,z;a,s) = 0 \tag{30}$$

$$\hat{u}_{zz}^{\mathrm{ring}}(r,\theta,z;a,s) = \frac{a}{\mu_0}\int_0^\infty \Omega_2(\xi,z;s;b)\xi J_0(a\xi)J_0(r\xi)\,\mathrm{d}\xi. \tag{31}$$

As $\gamma_1(\xi,z;s;b) = \gamma_1(\xi,s;z;b)$, $\gamma_3(\xi,z;s;b) = \gamma_2(\xi,s;z;b)$, $\Omega_2(\xi,z;s;b) = \Omega_2(\xi,s;z;b)$ and $\gamma_3(\xi,z;s;b) = \Omega_1(\xi,s;z;b)$, it follows that the foregoing Green's functions exhibit the characteristic spatial reciprocity, i.e. $\hat{u}_\beta^{\mathrm{ring}}(r,\theta,z;a,s) = \hat{u}_\beta^{\mathrm{ring}}(a,\theta,s;r,z)$ in the linear theory of elasticity.

3.4. *Uniform horizontal ring-load of radius* a *at* z = s

For a uniform, time-harmonic horizontal ring load of unit intensity acting in the $\theta = \theta_0$ direction, the load-induced stress discontinuities are

$$\tau_{r\theta}(r,\theta,s^-) - \tau_{r\theta}(r,\theta,s^+) = \cos(\theta-\theta_0)\delta(r-a) \tag{32}$$

$$\tau_{\theta\theta}(r,\theta,s^-) - \tau_{\theta\theta}(r,\theta,s^+) = -\sin(\theta-\theta_0)\delta(r-a). \tag{33}$$

From (32) and (33), one can easily deduce the Fourier components of the loading coefficients are

$$P_{\pm 1}(r;s) = \frac{e^{\pm i\theta_0}}{2}\delta(r-a) \tag{34}$$

$$Q_{\pm 1}(r;s) = \pm\frac{ie^{\pm i\theta_0}}{2}\delta(r-a), \tag{35}$$

with $P_m = Q_m = 0$ for $m \neq \pm 1$ and $R_m = 0$ for all m. For the foregoing asymmetric loading, the vertical, radial and angular components of the influence field can be expressed as

$$\hat{u}_{hr}^{ring}(r,\theta,z;a,s) = \frac{a\cos(\theta-\theta_0)}{2\mu_0}\left\{\int_0^\infty [\gamma_2(\xi,z;s;b)+\gamma_1(\xi,z;s;b)]\xi J_0(a\xi)J_0(r\xi)\,d\xi + \int_0^\infty [\gamma_2(\xi,z;s;b)-\gamma_1(\xi,z;s;b)]\xi J_0(a\xi)J_2(r\xi)\,d\xi\right\} \tag{36}$$

$$\hat{u}_{h\theta}^{ring}(r,\theta,z;a,s) = -\frac{a\sin(\theta-\theta_0)}{2\mu_0}\left\{\int_0^\infty [\gamma_2(\xi,z;s;b)+\gamma_1(\xi,z;s;b)]\xi J_0(a\xi)J_0(r\xi)\,d\xi - \int_0^\infty [\gamma_2(\xi,z;s;b)-\gamma_1(\xi,z;s;b)]\xi J_0(a\xi)J_2(r\xi)\,d\xi\right\} \tag{37}$$

$$\hat{u}_{hz}^{ring}(r,\theta,z;a,s) = \frac{a\cos(\theta-\theta_0)}{\mu_0}\left\{\int_0^\infty \Omega_1(\xi,z;s;b)\xi J_0(a\xi)J_1(r\xi)\,d\xi\right\}. \tag{38}$$

where the subscript h refers to the horizontal direction of the ring-load.

3.5. *Vertical point load at* r = 0, z = s

The vertical point-load Green's function can be derived from the results in Section 3.3 by considering a vertical ring-load of intensity $1/(2\pi a)$ and taking the limit of $a \to 0$. The result is the influence field for a unit internal vertical point-load in the form of

$$\hat{u}_{zr}^{Pt}(r,\theta,z;s) = -\frac{1}{2\pi\mu_0}\int_0^\infty \gamma_3(\xi,z;s;b)\xi J_1(r\xi)\,d\xi \tag{39}$$

$$\hat{u}_{z\theta}^{Pt}(r,\theta,z;s) = 0 \tag{40}$$

$$\hat{u}_{zz}^{Pt}(r,\theta,z;s) = \frac{1}{2\pi\mu_0}\int_0^\infty \Omega_2(\xi,z;s;b)\xi J_0(r\xi)\,d\xi. \tag{41}$$

3.6. *Horizontal point-load at* r = 0, z = s

Analogous to Section 3.5, the Green's functions for a unit horizontal point load acting at $z = s$, $r = 0$ in the $\theta = \theta_0$ direction can be obtained by considering Section 3.4 with a ring-load intensity of $1/(2\pi a)$ and taking the limit of $a \to 0$. The resulting influence field can be expressed as

$$\hat{u}_{hr}^{pt}(r,\theta,z;s)=\frac{\cos(\theta-\theta_0)}{4\pi\mu_0}\left\{\int_0^{\infty}[\gamma_2(\xi,z;s;b)+\gamma_1(\xi,z;s;b)]\xi J_0(r\xi)\,d\xi\right.$$
$$\left.+\int_0^{\infty}[\gamma_2(\xi,z;s;b)-\gamma_1(\xi,z;s;b)]\xi J_2(r\xi)\,d\xi\right\}. \tag{42}$$

$$\hat{u}_{h\theta}^{pt}(r,\theta,z;s)=-\frac{\sin(\theta-\theta_0)}{4\pi\mu_0}\left\{\int_0^{\infty}[\gamma_2(\xi,z;s;b)+\gamma_1(\xi,z;s;b)]\xi J_0(r\xi)\,d\xi\right.$$
$$\left.-\int_0^{\infty}[\gamma_2(\xi,z;s;b)-\gamma_1(\xi,z;s;b)]\xi J_2(r\xi)\,d\xi\right\}. \tag{43}$$

$$\hat{u}_{hz}^{pt}(r,\theta,z;s)=\frac{\cos(\theta-\theta_0)}{2\pi\mu_0}\left\{\int_0^{\infty}\Omega_1(\xi,z;s;b)\xi J_1(r\xi)\,d\xi\right\}. \tag{44}$$

4. EVALUATION OF THE GREEN'S FUNCTIONS

Owing to the complex behavior of the integrands which involve modified Bessel functions with frequency-dependent real and imaginary orders, a direct evaluation of the improper integrals in the influence fields (19)–(44) is difficult both analytically and numerically. The situation is further complicated by the expected singular behavior of some of the Green's functions. To deal with such problems, it is useful to employ the method of asymptotic decomposition (Pak, 1987) wherein the leading asymptotic expansions of the featured integrands (responsible for singular behavior) are extracted and integrated analytically so that the remaining parts with strong decay can be evaluated numerically. Mathematically, one may write

$$\hat{u}_{ij}^{*}=(\hat{u}_{ij}^{*})_1+(\hat{u}_{ij}^{*})_2. \tag{45}$$

In (45), superscript * stands for ring or pt, while the subscripts 1 and 2 denote the analytically and numerically evaluated parts of the influence fields, respectively. To illustrate the approach, the evaluation procedure for some Green's functions will be presented in this section. Analogous treatment can be developed for the rest of the influence fields.

4.1. *Analytically evaluated parts of influence fields*

By virtue of the asymptotic expansions of modified Bessel functions with large arguments and fixed complex orders

$$K_\nu(x)\sim\sqrt{\frac{\pi}{2x}}e^{-x}\left\{1+\frac{4\nu^2-1}{8x}+\frac{(4\nu^2-1)(4\nu^2-9)}{2!(8x)^2}+\frac{(4\nu^2-1)(4\nu^2-9)(4\nu^2-25)}{3!(8x)^3}\right.$$
$$\left.+\frac{(4\nu^2-1)(4\nu^2-9)(4\nu^2-25)(4\nu^2-49)}{4!(8x)^4}\right\},\quad |\mathrm{Arg}(x)|<\tfrac{3}{2}\pi \tag{46}$$

$$I_\nu(x)\sim\frac{e^x}{\sqrt{2\pi x}}\left\{1-\frac{4\nu^2-1}{8x}+\frac{(4\nu^2-1)(4\nu^2-9)}{2!(8x)^2}-\frac{(4\nu^2-1)(4\nu^2-9)(4\nu^2-25)}{3!(8x)^3}\right.$$
$$\left.+\frac{(4\nu^2-1)(4\nu^2-9)(4\nu^2-25)(4\nu^2-49)}{4!(8x)^4}\right\},\quad |\mathrm{Arg}(x)|<\tfrac{1}{2}\pi, \tag{47}$$

the leading asymptotic behavior of the functions γ_1, γ_2, γ_3, Ω_1 and Ω_2 as $\xi\to\infty$ can be written as

$$\gamma_1^{\text{asym.}}(\xi, z; s; b) = \frac{C}{\xi}\{e^{-\xi(z+s)}[2-2(z+s)\xi+2zs\xi^2]+e^{-\xi|z-s|}[2-|z-s|\xi]\} \tag{48}$$

$$\gamma_2^{\text{asym.}}(\xi, z; s; b) = \frac{3C}{\xi}\{e^{-\xi(z+s)}+e^{-\xi|z-s|}\} \tag{49}$$

$$\gamma_3^{\text{asym.}}(\xi, z; s; b) = \frac{C}{\xi}\{e^{-\xi(z+s)}[2-2(z-s)\xi-2zs\xi^2]+e^{-\xi|z-s|}[(s-z)\xi]\} \tag{50}$$

$$\Omega_1^{\text{asym.}}(\xi, z; s; b) = \frac{C}{\xi}\{e^{-\xi(z+s)}[2-2(s-z)\xi-2zs\xi^2]+e^{-\xi|z-s|}[(z-s)\xi]\} \tag{51}$$

$$\Omega_2^{\text{asym.}}(\xi, z; s; b) = \frac{C}{\xi}\{e^{-\xi(z+s)}[2+2(z+s)\xi+2zs\xi^2]+e^{-\xi|z-s|}[2+|z-s|\xi]\}, \tag{52}$$

where

$$C = \frac{1}{6(1+bz)(1+bs)} \tag{53}$$

Being also the parts of the integrands which cause the singular behaviors of the Green's functions of interest, the foregoing asymptotic representations are independent of frequency and are identical to those for the corresponding static problem. With (48)–(52), the first part of the featured influence fields can be expressed as

$$\begin{aligned}(\hat{u}_{rr}^{\text{ring}})_1(r, \theta, z; a, s) &= \frac{a}{\mu_0}\int_0^\infty \gamma_1^{\text{asym.}}(\xi, z; s; b)\xi J_1(a\xi)J_1(r\xi)\,\mathrm{d}\xi \\ &= \frac{aC}{\mu_0}\{\tfrac{5}{2}\mathcal{I}_2(1,1,0)-2(z+s)\mathcal{I}_2(1,1,1) \\ &\quad +2zs\mathcal{I}_2(1,1,2)+2\mathcal{I}_1(1,1,0)-|z-s|\mathcal{I}_1(1,1,1)\}\end{aligned} \tag{54}$$

$$\begin{aligned}(\hat{u}_{rz}^{\text{ring}})_1(r, \theta, z; a, s) &= -\frac{a}{\mu_0}\int_0^\infty \Omega_1^{\text{asym.}}(\xi, z; s; b)\xi J_1(a\xi)J_0(r\xi)\,\mathrm{d}\xi \\ &= -\frac{aC}{\mu_0}\{\tfrac{3}{2}\mathcal{I}_2(0,1,0)-2(s-z)\mathcal{I}_2(0,1,1) \\ &\quad -2zs\mathcal{I}_2(0,1,2)+(z-s)\mathcal{I}_1(0,1,1)\}\end{aligned} \tag{55}$$

$$\begin{aligned}(\hat{u}_{zr}^{\text{ring}})_1(r, \theta, z; a, s) &= -\frac{a}{\mu_0}\int_0^\infty \gamma_3^{\text{asym.}}(\xi, z; s; b)\xi J_0(a\xi)J_1(r\xi)\,\mathrm{d}\xi \\ &= -\frac{aC}{\mu_0}\{\tfrac{3}{2}\mathcal{I}_2(1,0,0)-2(z-s)\mathcal{I}_2(1,0,1) \\ &\quad -2zs\mathcal{I}_2(1,0,2)+(s-z)\mathcal{I}_1(1,0,1)\}\end{aligned} \tag{56}$$

$$\begin{aligned}(\hat{u}_{zz}^{\text{ring}})_1(r, \theta, z; a, s) &= \frac{a}{\mu_0}\int_0^\infty \Omega_2^{\text{asym.}}(\xi, z; s; b)\xi J_0(a\xi)J_0(r\xi)\,\mathrm{d}\xi \\ &= \frac{aC}{\mu_0}\{\tfrac{5}{2}\mathcal{I}_2(0,0,0)+2(z+s)\mathcal{I}_2(0,0,1) \\ &\quad +2zs\mathcal{I}_2(0,0,2)+2\mathcal{I}_1(0,0,0)+|z-s|\mathcal{I}_1(0,0,1)\}\end{aligned} \tag{57}$$

$$(\hat{u}_{hr}^{pt})_1(r,\theta,z;s) = \frac{\cos(\theta-\theta_0)}{4\pi\mu_0}\left\{\int_0^\infty [\gamma_2^{asym}(\xi,z;s;b)+\gamma_1^{asym}(\xi,z;s;b)]\xi J_0(r\xi)\,d\xi \right.$$
$$\left. + \int_0^\infty [\gamma_2^{asym}(\xi,z;s;b)-\gamma_1^{asym}(\xi,z;s;b)]\xi J_2(r\xi)\,d\xi\right\}$$
$$= \frac{C\cos(\theta-\theta_0)}{4\pi\mu_0}\left\{\tfrac{1}{2}\mathcal{I}_2(0,0)-2(z+s)\mathcal{I}_2(0,1)\right.$$
$$+2zs\mathcal{I}_2(0,2)+5\mathcal{I}_1(0,0)-|z-s|\mathcal{I}_1(0,1)$$
$$+\tfrac{1}{2}\mathcal{I}_2(2,0)+2(z+s)\mathcal{I}_2(2,1)$$
$$\left.-2zs\mathcal{I}_2(2,2)+\mathcal{I}_1(2,0)+|z-s|\mathcal{I}_1(2,1)\right\} \tag{58}$$

$$(\hat{u}_{hz}^{pt})_1(r,\theta,z;s) = \frac{\cos(\theta-\theta_0)}{2\pi\mu_0}\left\{\int_0^\infty \Omega_1^{asym}(\xi,z;s;b)\xi J_1(r\xi)\,d\xi\right\}$$
$$= \frac{C\cos(\theta-\theta_0)}{2\pi\mu_0}\left\{\tfrac{1}{2}\mathcal{I}_2(1,0)-2(s-z)\mathcal{I}_2(1,1)\right.$$
$$\left.-2zs\mathcal{I}_2(1,2)+(z-s)\mathcal{I}_1(1,1)\right\}, \tag{59}$$

where

$$\mathcal{I}_k(m,n,l) \equiv \mathcal{I}(m,n,l,r,a,d_k) = \int_0^\infty J_m(r\xi)J_n(a\xi)\,e^{-d_k\xi}\xi^l\,d\xi, \tag{60}$$

$$\mathcal{J}_k(m,l) \equiv \mathcal{J}(m,l,r,d_k) = \int_0^\infty J_m(r\xi)\,e^{-d_k\xi}\xi^l\,d\xi \tag{61}$$

$$d_1 = |z-s|, \quad d_2 = z+s. \tag{62}$$

Analytical expressions for the required integrals in (60) and (61) are listed in Appendix B. It should be noted that the integrals of the form (60) are expressible in terms of complete elliptic integrals [see Eason *et al.* (1955)], while those in (61) can be written in terms of closed-form algebraic functions (Erdelyi, 1954). Analogous to the case for a homogeneous solid, it can be shown that $(\hat{u}_{rr}^{ring})_1$ and $(\hat{u}_{zz}^{ring})_1$ are logarithmically singular as $r \to a$ and $z \to s$, while $(\hat{u}_{hr}^{pt})_1$ is Cauchy singular as $r \to 0$ and $z \to s$. In contrast, Green's functions $\hat{u}_{rz}^{ring}$, $\hat{u}_{zr}^{ring}$ and $\hat{u}_{hz}^{pt}$ exhibit no singularities.

4.2. *Numerically evaluated parts of influence fields*

As mentioned earlier, the residual integrands in the integral representation of the Green's functions $(\hat{u}_{ij}^{*})_2$ are composed of regular functions. By design, they also decay quickly with ξ owing to the asymptotic extraction. As a result, the residual semi-infinite integrals can be evaluated numerically with a suitable truncation of the integration interval. For convenience, the integration is performed in terms of the auxiliary variable $\zeta = \xi/b$, which is the natural choice considering the form of the functions γ_1, γ_2, γ_3, Ω_1 and Ω_2 [see (A1)–(A5)]. These functions have generally a number of poles along the formal path of inversion integrals in the complex ζ-plane due to the zeros of their denominator $\Delta(\zeta)$ defined in (A13). By virtue of the analyticity of the integrands, the path of integration can be deformed into the upper half-plane to avoid the singularities on these occasions. In the selection of such modified paths, however, the following observations are pertinent.

With the dimensionless frequency $\bar{\omega}$ defined as

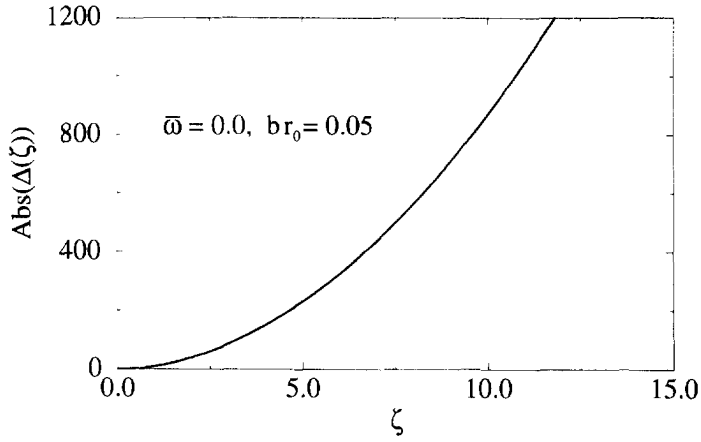

Fig. 1. Behavior of the denominator $\Delta(\zeta)$ for small values of $\bar{\omega}/(br_0)$.

$$\bar{\omega} = \frac{\omega r_0}{\sqrt{(\mu_0/\rho)}}, \tag{63}$$

where r_0 is a characteristic length, one may observe that both radicals α and β are real-valued for $\bar{\omega}/(br_0) < 1/2$. In this case, Abs($\Delta(\zeta)$) monotonically increases along the real axis, starting from zero at $\zeta = 0$ (see Fig. 1). It can be shown by a limit analysis that the featured integrands are all regular at $\zeta = 0$. Consequently, for $\bar{\omega}/(br_0) < 1/2$, there are no poles along the formal path of integration. By virtue of the Cauchy theorem in the theory of complex variables, one may thus deduce that the imaginary part of the kernels in (19)–(44) and, therefore, of the respective displacement influence fields will be identically zero, i.e. no radiation damping. Physically this means the existence of a cutoff frequency. The same phenomenon was observed by Gladwell (1964) in his study of the forced torsional vibrations on an elastic stratum resting on a rigid base, and by Guzina (1992) in the study of dynamic response of the surface footing resting on a heterogeneous half-space. The reason for the existence of the cutoff frequency in a heterogeneous half-space is discussed in Nettleton (1940) who observed that wave rays in such media are generally curved. In particular, for soils with a linearly varying velocity, the wave will follow a circular path, as shown in Fig. 2. Thus total reflection of waves is possible and does not require the presence of a discontinuity in the elastic properties of the medium. Note that the circular wave paths imply that one will find spherical wave fronts as in the homogeneous case, although their centers are shifted downwards as the wave propagates through the medium.

For $\bar{\omega}/(br_0) > 1/2$, the typical behavior of the function $\Delta(\zeta)$ is presented in Fig. 3. As the ratio $\bar{\omega}/(br_0)$ increases, orders α and β (of the Bessel functions) become imaginary, and multiple poles start to appear along the formal path of integration, i.e. the positive real ζ-axis. The phenomenon of multiple poles was also found by Gladwell (1964) in the case of torsional vibrations on a homogeneous stratum. Furthermore, it is observed that with

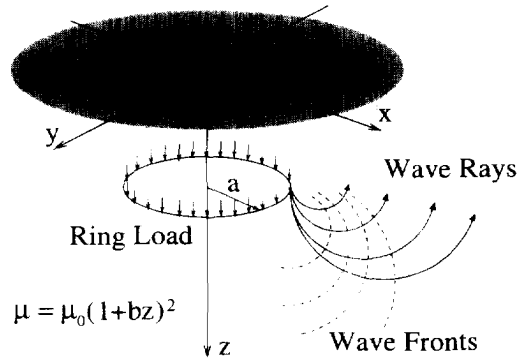

Fig. 2. Wave propagation in heterogeneous media.

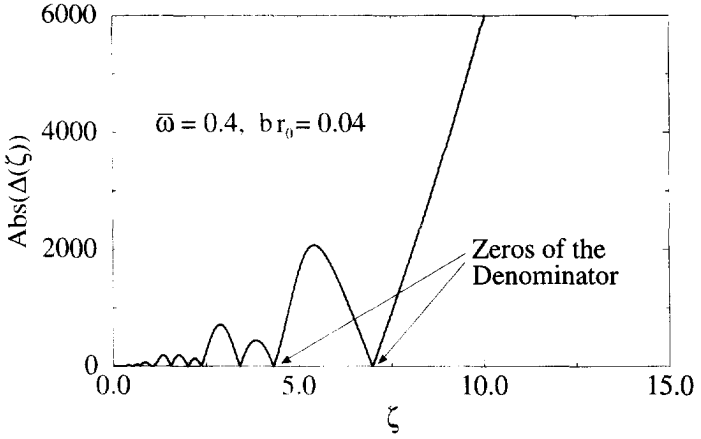

Fig. 3. Behavior of the denominator $\Delta(\zeta)$ for large values of $\bar{\omega}\,(br_0)$.

increasing $\bar{\omega}\,(br_0)$, the number of the poles would increase and their positions along the path of integration would move to the right. As an upper bound for the position of the pole furthest from the origin ($\zeta = 0$), one may adopt the location of the Rayleigh pole for the homogeneous medium with $\lambda = \mu = \mu_0$, i.e.

$$\zeta^* = \frac{k_R}{b} \approx 1.088\,\frac{\bar{\omega}}{br_0}. \tag{64}$$

Physically, the above statement describes the lower bound for the phase velocities in the heterogeneous medium characterized by (1) as the Rayleigh wave speed in its 'uppermost layer', $\mu = \mu_0$. In fact, as the ratio $\bar{\omega}\,(br_0)$ increases, changes in the medium properties over the wave length become smaller and the actual position of the pole furthest from the origin approaches ζ^* from the left.

Prompted by (64), the length of the modified path with respect to ζ is chosen to be $d = 1.0 + 1.1\bar{\omega}\,(br_0)$. Furthermore, the modified path of integration should not be too close to the real axis to avoid oscillatory behavior, nor too far from it to preserve the analyticity of the integrand. The resulting route is presented in Fig. 4.

5. ILLUSTRATIVE RESULTS

By means of the foregoing mathematical analysis and computational scheme, the dynamic Green's functions for the vertically heterogeneous medium can be evaluated numerically. In what follows, a set of numerical results will be presented for illustrative purposes. To normalize the results, the characteristic length r_0 is chosen to correspond to the radius of the ring load and the embedment depth of the point-load, respectively.

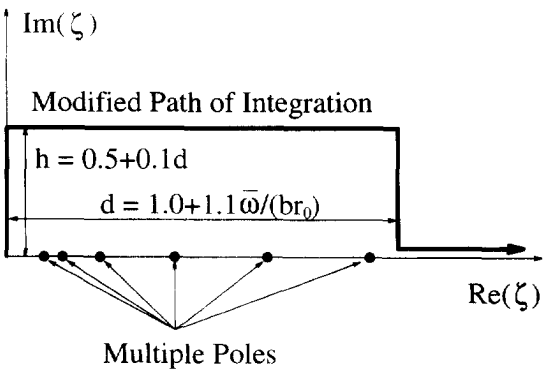

Fig. 4. Modified path of integration.

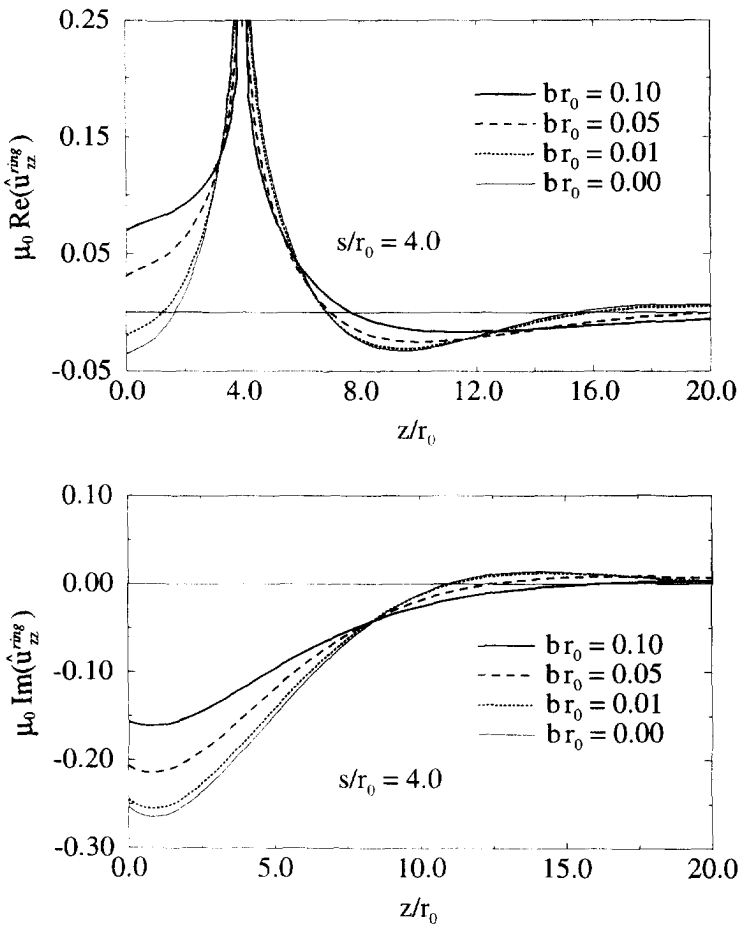

Fig. 5. Ring-load Green's function $\hat{u}^{ring}$, $r = a$, $\bar{\omega} = 0.5$.

In Fig. 5, the real and imaginary parts of the Green's function $\hat{u}_{zz}^{ring}$ with $s = 4a$ are plotted versus depth along the surface $r = a$ for a dimensionless frequency $\bar{\omega} = 0.5$. Results are presented for three different values of the heterogeneity rate in the range $0.01 \leqslant br_0 \leqslant 0.10$, together with the numerical results of the homogeneous half-space formulation, denoted by '$br_0 = 0.00$'. From the display, it is apparent that as b decreases to zero, both the real and imaginary parts of the Green's function approach the corresponding solution for a homogeneous half-space. As expected, the real part of $\hat{u}_{zz}^{ring}$ exhibits a logarithmic singularity at $z = s$ and $r = a$, while its imaginary part remains regular throughout. It can be also observed from Fig. 5 that the wave length increases and the imaginary part diminishes with a higher value of b which means a stiffer medium. In fact, for a sufficiently high b, the cutoff frequency would reach the prescribed frequency of excitation, rendering the imaginary part of the response zero. In Fig. 6, the foregoing Green's function is plotted versus the radial coordinate on the horizontal plane $z = s$. Comparison with the previous figure reveals that the displacement field has a slower decay in the radial direction than in the z-direction along which the modulus increases.

The response of the medium due to a time-harmonic radial ring-source located at $s = 4a$ with $\bar{\omega} = 0.5$ is illustrated in Fig. 7, where $\hat{u}_{rr}^{ring}$ is plotted as a function of the radius at $z = s$. As a self-equilibrating buried source, the Green's function $\hat{u}_{rr}^{ring}$ is characterized by a more localized response at the neighborhood $r = a$. In addition, one may note that

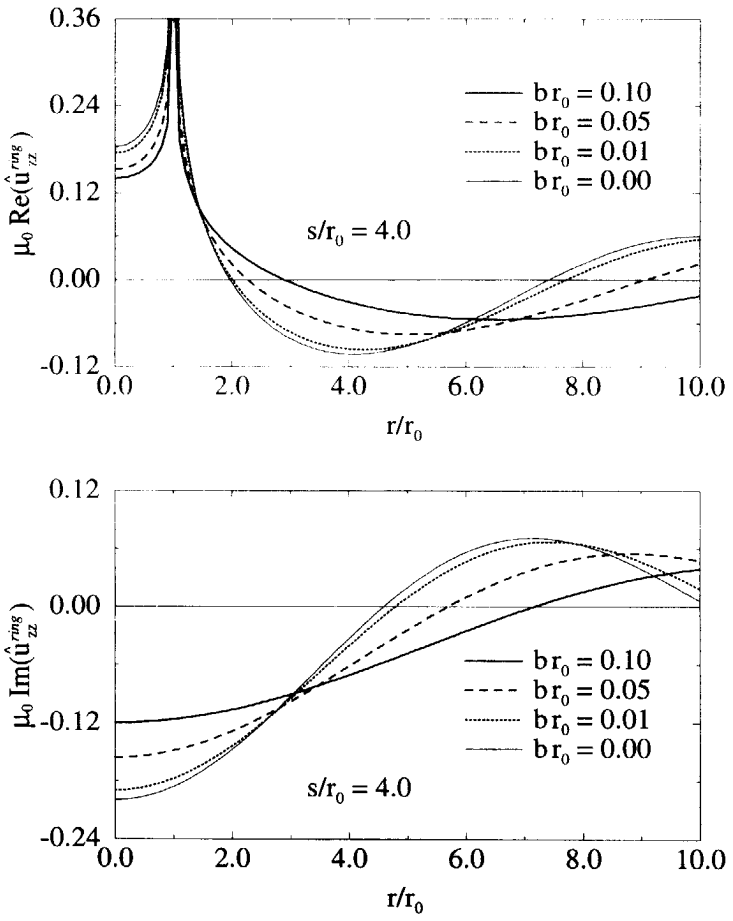

Fig. 6. Ring-load Green's function $\hat{u}_{zz}^{\mathrm{ring}}$, $z = s$, $\bar{\omega} = 0.5$.

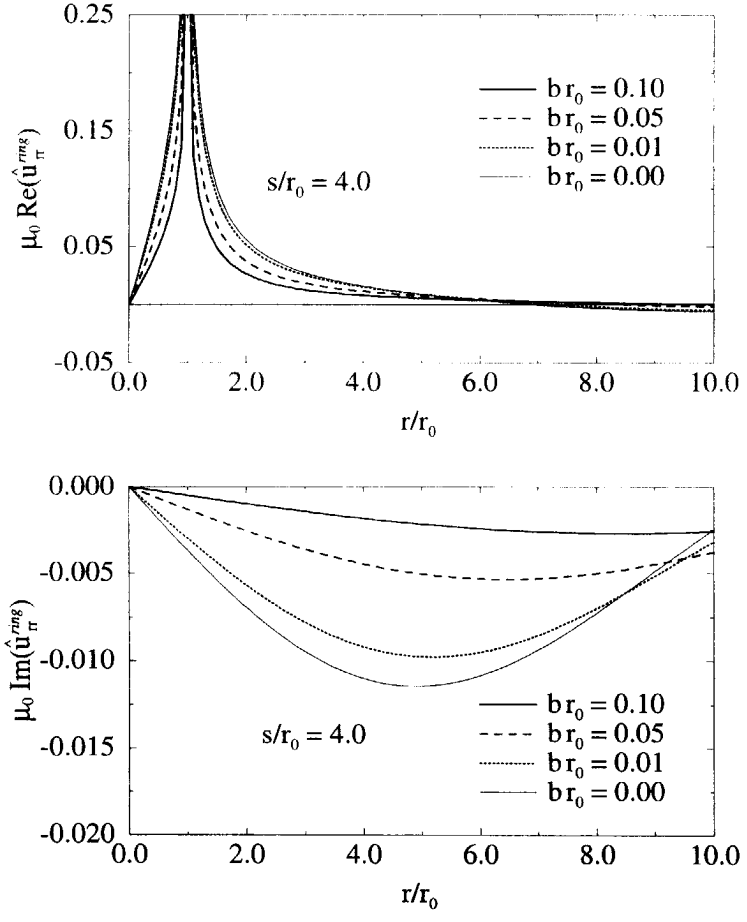

Fig. 7. Ring-load Green's function $\hat{u}_{rr}^{\mathrm{ring}}$, $z = s$, $\bar{\omega} = 0.5$.

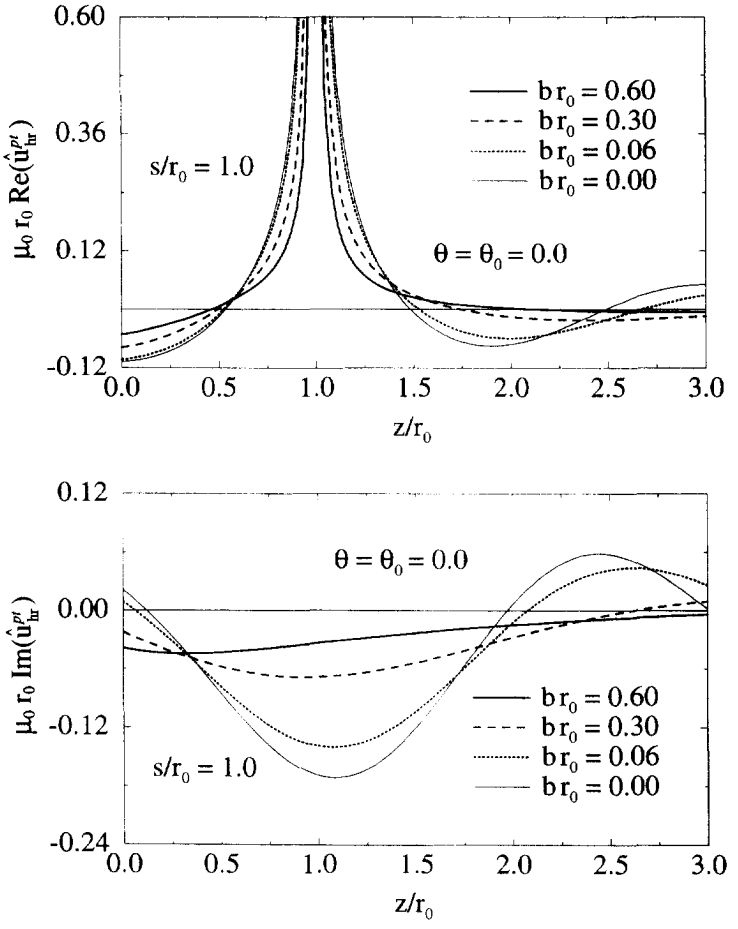

Fig. 8. Point-load Green's function $\hat{u}^{pt}_{hr}$, $r = 0$, $\bar{\omega} = 3.0$.

$\hat{u}^{ring}_{rr}(0, z; a, s) = 0$, i.e. the radial component of the Green's function vanishes at $r = 0$, which is in accordance with the axial symmetry of the problem.

Finally, the asymmetric Green's function $\hat{u}^{pt}_{hr}$ due to a horizontal point-load acting in the $\theta_0 = 0$ direction with $\bar{\omega} = 3.0$ is presented in Fig. 8. Taking s to be r_0, the response is plotted along the z-axis for $\theta = 0$. Similar to the previous results, a decrease in the heterogeneity parameter b is accompanied by a reduction of the wave length and an increase in the magnitude of the displacements. Not surprisingly, the difference between the numerical solutions for a homogeneous ($br_0 = 0.00$) and a weakly heterogeneous ($br_0 = 0.06$) medium is found to be small at points close to the free-surface, where the two solids have the same modulus. By virtue of expression (58), the real component of the Green's function always exhibits a Cauchy-singular behavior with the response becoming more localized with increasing b. In other words, the singular character of the Green's function is not affected by the spatial variations in the medium properties.

6. CONCLUSIONS

In this paper, the three-dimensional response of a smoothly heterogeneous elastic half-space due to a variety of time-harmonic ring- and point-sources is presented. The evaluation of these Green's functions on the basis of decomposition into analytical and residual parts is described in detail. The analytical parts for the ring- and point-load Green's functions are found to be expressible in terms of the elliptic integrals and algebraic functions, respectively. The residual regular parts of the Green's functions can be evaluated by the method of numerical contour integration. A set of numerical results is presented and compared to the solutions for a uniform half-space, highlighting the characteristic features

of wave propagation in media whose modulus increases continuously with depth. These fundamental solutions can be directly incorporated into various boundary integral equation methods for relevant boundary-value problems in solid and geo-mechanics. With the aid of Fourier or Laplace transforms, the present solutions can be readily extended to the treatment of transient problems.

Acknowledgement – The support from the National Science Foundation through Grant BCS-8958402 to R.Y.S.P. is gratefully acknowledged.

REFERENCES

Apsel, J. R. (1979). Dynamic Green's functions for layered media and applications to boundary value problems. Ph.D. Thesis, University of California, San Diego.

Banerjee, P. K. and Mamoon, S. M. (1990). A fundamental solution due to a periodic point force in the interior of an elastic half-space. *Earthquake Engng Structural Dynamics* **19,** 91–105.

Brebbia, C. A., Telles, J. C. F. and Wrobel, L. C. (1984). *Boundary Element Techniques: Theory and Applications in Engineering*. Springer, New York.

Eason, G., Noble, B. and Sneddon, I. N. (1955). On certain integrals of Lipschitz–Hankel type involving products of Bessel functions. *Philos. Trans. R. Soc. Lond. Series A* **247,** 529–551.

Erdelyi, A. (Ed.) (1954). *Tables of Integral Transforms*, Vol. 2. McGraw-Hill, New York.

Gladwell, G. M. L. (1964). The forced torsional vibration of an elastic stratum. *Int. J. Engng Sci.* **7,** 1011–1024.

Guzina, B. B. (1992). Dynamic response of surface foundations on heterogeneous soils. M. S. Thesis, University of Colorado, Boulder.

Hardin, B. O. and Drnevich, V. P. (1972). Shear modulus and damping in soils: design equations and curves. *J. Soil Mech. Foundation Engng Div. Am. Soc. Civil Engineers* **98,** 668–692.

Nettleton, L. L. (1940). *Geophysical Prospecting for Oil*. McGraw-Hill, New York.

Pak, R. Y. S. (1987). Asymmetric wave propagation in a half-space by a method of potentials. *J. Appl. Mech., Am. Soc. Mech. Engineers* **54,** 121–126.

Pak, R. Y. S. and Guzina, B. B. (1995). Three-dimensional wave propagation analysis of a smoothly heterogeneous solid. *J. Mech. Phys. Solids* **43,** 533–551.

Pak, R. Y. S. and Ji, F. (1994). Mathematical boundary integral analysis of an embedded shell under dynamic excitations. *Int. J. Num. Meth. Engng* **37,** 2501–2520.

APPENDIX A: KERNEL FUNCTIONS

$$
\begin{aligned}
\Gamma_{\beta}(\zeta, z; x, b) = {} & H(z-\zeta)\frac{x^{\beta+1}\zeta^{\beta}}{b(\beta+\tfrac{1}{4}-3\gamma^2)}\left\{I_{\beta}(x)K_{\beta}(y)\right. \\
& \left. + I_{\beta}(x)K_{\beta+1}(y)\left[\frac{2\beta+5}{2x}+\frac{I_{\beta-1}(x)}{I_{\beta}(x)}\right]\left[\frac{2\beta+5}{2y}\frac{K_{\beta}(y)}{K_{\beta+1}(y)}-1\right]\right\} \\
& + \frac{x^{\beta+1}\zeta^{\beta}}{b(\beta+\tfrac{1}{4}-3\gamma^2)\Delta(\zeta)}\left\{\frac{K_{\beta}(x)}{K_{\beta+1}(\zeta)}I_{\beta}(\zeta)K_{\beta}(y)\right. \\
& \left[-\left(f_1\frac{K_{\beta}(\zeta)}{K_{\beta+1}(\zeta)}+f_2\right)+\left(f_3\frac{K_{\beta}(\zeta)}{K_{\beta+1}(\zeta)}+f_4\right)\frac{I_{\beta+1}(\zeta)}{I_{\beta}(\zeta)}\right] \\
& + \frac{K_{\beta+1}(x)}{K_{\beta+1}(\zeta)}I_{\beta}(\zeta)K_{\beta+1}(y)\left[\frac{2\beta+5}{2x}\frac{K_{\beta}(x)}{K_{\beta+1}(x)}-1\right]\left[\frac{2\beta+5}{2y}\frac{K_{\beta}(y)}{K_{\beta+1}(y)}-1\right] \\
& \left[-\left(f_1\frac{K_{\beta}(\zeta)}{K_{\beta+1}(\zeta)}+f_2\right)+\left(f_3\frac{K_{\beta}(\zeta)}{K_{\beta+1}(\zeta)}+f_4\right)\frac{I_{\beta+1}(\zeta)}{I_{\beta}(\zeta)}\right] \\
& + f_3\frac{K_{\beta}(x)}{K_{\beta+1}(\zeta)}\frac{K_{\beta+1}(y)}{K_{\beta+1}(\zeta)}\left[\frac{2\beta+5}{2y}\frac{K_{\beta}(y)}{K_{\beta+1}(y)}-1\right] \\
& \left.+f_3\frac{K_{\beta}(y)}{K_{\beta+1}(\zeta)}\frac{K_{\beta+1}(x)}{K_{\beta+1}(\zeta)}\left[\frac{2\beta+5}{2x}\frac{K_{\beta}(x)}{K_{\beta+1}(x)}-1\right]\right\} \\
& - H(z-x)\frac{x^{\beta+1}\zeta^{\beta}}{b(\beta+\tfrac{1}{4}-3\gamma^2)}\left\{I_{\beta}(y)K_{\beta}(x)\right. \\
& \left.+I_{\beta}(y)K_{\beta+1}(x)\left[\frac{2\beta+5}{2y}+\frac{I_{\beta-1}(y)}{I_{\beta}(y)}\right]\left[\frac{2\beta+5}{2x}\frac{K_{\beta}(x)}{K_{\beta+1}(x)}-1\right]\right\}
\end{aligned}
\tag{A1}
$$

$$\gamma_2(\xi,z;x,b) = H(x-z)\frac{x^{\alpha+\beta}y^{\beta+2}\zeta}{b}\{I_\beta(x)K_\beta(y)\}$$
$$+\frac{x^{\alpha+\beta}y^{\beta+2}\zeta}{b\left\{(\beta+\tfrac{1}{2})\dfrac{K_\beta(\zeta)}{K_{\beta+1}(\zeta)}-\zeta\right\}}\left\{\frac{K_\beta(x)}{K_{\beta+1}(\zeta)}I_\beta(\zeta)K_\beta(y)\left[\beta-\tfrac{1}{2}+\zeta\frac{I_{\beta+1}(\zeta)}{I_\beta(\zeta)}\right]\right\}$$
$$+H(z-x)\frac{x^{\alpha+\beta}y^{\beta+2}\zeta}{b}I_\beta(y)K_\beta(x) \tag{A2}$$

$$\gamma_3(\xi,z;x,b) = H(x-z)\frac{x^{\alpha+\beta+2}\zeta}{b(\alpha_4-3\alpha^2)}\left\{I_\beta(x)K_{\beta+1}(y)\left[\frac{2\alpha-3}{2\alpha}\frac{K_\beta(y)}{K_{\beta+1}(y)}-1\right]\right.$$
$$\left.-I_\beta(x)K_\beta(y)\left[\frac{2\beta+5}{2\alpha}+\frac{I_{\beta+1}(x)}{I_\beta(x)}\right]\right\}$$
$$+\frac{x^{\alpha+\beta}y^{\beta+2}\zeta}{b(\alpha_4-3\alpha^2)\Delta(\zeta)}\left\{\frac{K_{\beta+1}(y)}{K_{\beta+1}(\zeta)}I_\beta(\zeta)K_\beta(x)\left[\frac{2\alpha-3}{2\alpha}\frac{K_\beta(y)}{K_{\beta+1}(y)}-1\right]\right.$$
$$\left.\left[-\left(t_1\frac{K_\beta(\zeta)}{K_{\beta+1}(\zeta)}+t_2\right)+\left(t_3\frac{K_\beta(\zeta)}{K_{\beta+1}(\zeta)}+t_4\right)\frac{I_{\beta+1}(\zeta)}{I_\beta(\zeta)}\right]\right.$$
$$-\frac{K_\beta(x)}{K_{\beta+1}(\zeta)}I_\beta(\zeta)K_{\beta+1}(y)\left[\frac{2\beta+5}{2\alpha}\frac{K_\beta(y)}{K_{\beta+1}(y)}-1\right]$$
$$\left.\left[-\left(t_1\frac{K_\beta(\zeta)}{K_{\beta+1}(\zeta)}+t_2\right)+\left(t_3\frac{K_\beta(\zeta)}{K_{\beta+1}(\zeta)}+t_4\right)\frac{I_{\beta+1}(\zeta)}{I_\beta(\zeta)}\right]\right.$$
$$+t_5\frac{K_\beta(y)}{K_{\beta+1}(\zeta)}\frac{K_\beta(x)}{K_{\beta+1}(\zeta)}$$
$$\left.+t_6\frac{K_{\beta+1}(y)}{K_{\beta+1}(\zeta)}\frac{K_{\beta+1}(x)}{K_{\beta+1}(\zeta)}\left[\frac{2\alpha-3}{2\alpha}\frac{K_\beta(y)}{K_{\beta+1}(y)}-1\right]\left[\frac{2\beta+5}{2\alpha}\frac{K_\beta(x)}{K_{\beta+1}(x)}-1\right]\right\}$$
$$-H(z-x)\frac{x^{\beta+1}y^{\beta+2}\zeta}{b(\alpha_4-3\alpha^2)}\left\{I_\beta(y)K_\beta(x)\left[\frac{2\alpha-3}{2\alpha}+\frac{I_{\beta+1}(y)}{I_\beta(y)}\right]\right.$$
$$\left.+I_\beta(y)K_\beta(x)\left[\frac{2\beta+5}{2\alpha}\frac{K_\beta(x)}{K_{\beta+1}(x)}-1\right]\right\}, \tag{A3}$$

$$\Omega_3(\xi,z;x,b) = H(x-z)\frac{x^{\beta+1}y^{\beta+2}\zeta}{b(\alpha_4-3\alpha^2)}\left\{I_\beta(x)K_\beta(y)\left[\frac{2\alpha-3}{2\alpha}+\frac{I_{\beta+1}(x)}{I_\beta(x)}\right]\right.$$
$$\left.+I_\beta(x)K_{\beta+1}(y)\left[\frac{2\beta-5}{2\alpha}\frac{K_\beta(y)}{K_{\beta+1}(y)}-1\right]\right\}$$
$$+\frac{x^{\beta+1}y^{\beta+2}\zeta}{b(\alpha_4-3\alpha^2)\Delta(\zeta)}\left\{\frac{K_{\beta+1}(x)}{K_{\beta+1}(\zeta)}I_\beta(\zeta)K_\beta(y)\left[\frac{2\alpha-3}{2\alpha}\frac{K_\beta(x)}{K_{\beta+1}(x)}-1\right]\right.$$
$$\left.\left[-\left(t_1\frac{K_\beta(\zeta)}{K_{\beta+1}(\zeta)}+t_2\right)+\left(t_3\frac{K_\beta(\zeta)}{K_{\beta+1}(\zeta)}+t_4\right)\frac{I_{\beta+1}(\zeta)}{I_\beta(\zeta)}\right]\right.$$
$$-\frac{K_\beta(x)}{K_{\beta+1}(\zeta)}I_\beta(\zeta)K_{\beta+1}(y)\left[\frac{2\beta+5}{2\alpha}\frac{K_\beta(y)}{K_{\beta+1}(y)}-1\right]$$
$$\left.\left[-\left(t_1\frac{K_\beta(\zeta)}{K_{\beta+1}(\zeta)}+t_2\right)+\left(t_3\frac{K_\beta(\zeta)}{K_{\beta+1}(\zeta)}+t_4\right)\frac{I_{\beta+1}(\zeta)}{I_\beta(\zeta)}\right]\right.$$
$$+t_5\frac{K_\beta(x)}{K_{\beta+1}(\zeta)}\frac{K_\beta(y)}{K_{\beta+1}(\zeta)}$$
$$\left.+t_6\frac{K_{\beta+1}(x)}{K_{\beta+1}(\zeta)}\frac{K_{\beta+1}(y)}{K_{\beta+1}(\zeta)}\left[\frac{2\alpha-3}{2\alpha}\frac{K_\beta(x)}{K_{\beta+1}(x)}-1\right]\left[\frac{2\beta+5}{2\alpha}\frac{K_\beta(y)}{K_{\beta+1}(y)}-1\right]\right\}$$
$$+H(z-x)\frac{x^{\beta+1}y^{\beta+2}\zeta}{b(\alpha_4-3\alpha^2)}\left\{I_\beta(y)K_{\beta+1}(x)\left[\frac{2\alpha-3}{2\alpha}\frac{K_\beta(x)}{K_{\beta+1}(x)}-1\right]\right.$$
$$\left.+I_\beta(y)K_\beta(x)\left[\frac{2\beta+5}{2\alpha}+\frac{I_{\beta+1}(y)}{I_\beta(y)}\right]\right\} \tag{A4}$$

and

$$\Omega_2(\xi, z, s; b) = H(s-z)\frac{x^{\frac{1}{2}}y^{-\frac{1}{2}}e^{-\zeta}}{b(\frac{27}{4}-3\alpha^2)}\left\{I_\beta(x)K_\beta(y)\right.$$
$$\left.+I_\alpha(x)K_{\alpha-1}(y)\left[\frac{2\alpha-3}{2x}+\frac{I_{\alpha+1}(x)}{I_\alpha(x)}\right]\left[\frac{2\alpha-3}{2y}\frac{K_\alpha(y)}{K_{\alpha+1}(y)}-1\right]\right\}$$
$$+\frac{x^{\frac{1}{2}}y^{-\frac{1}{2}}e^{-\zeta}}{b(\frac{27}{4}-3\alpha^2)\Delta(\zeta)}\left\{\frac{K_\beta(x)}{K_{\beta-1}(\zeta)}I_\beta(\zeta)K_\beta(y)\right.$$
$$\left[-\left(f_1\frac{K_\alpha(\zeta)}{K_{\alpha-1}(\zeta)}+f_3\right)+\left(f_2\frac{K_\alpha(\zeta)}{K_{\alpha+1}(\zeta)}+f_4\right)\frac{I_{\beta+1}(\zeta)}{I_\beta(\zeta)}\right]$$
$$+\frac{K_{\alpha-1}(x)}{K_{\alpha-1}(\zeta)}I_\alpha(\zeta)K_{\alpha-1}(y)\left[\frac{2\alpha-3}{2x}\frac{K_\alpha(x)}{K_{\alpha-1}(x)}-1\right]\left[\frac{2\alpha-3}{2y}\frac{K_\alpha(y)}{K_{\alpha-1}(y)}-1\right]$$
$$\left[-\left(f_1\frac{K_\beta(\zeta)}{K_{\beta-1}(\zeta)}+f_3\right)+\left(f_2\frac{K_\beta(\zeta)}{K_{\beta+1}(\zeta)}+f_4\right)\frac{I_{\alpha+1}(\zeta)}{I_\alpha(\zeta)}\right]$$
$$+f_5\frac{K_\beta(x)}{K_{\beta-1}(\zeta)}\frac{K_{\alpha-1}(y)}{K_{\alpha-1}(\zeta)}\left[\frac{2\alpha-3}{2y}\frac{K_\alpha(y)}{K_{\alpha+1}(y)}-1\right]$$
$$\left.+f_5\frac{K_\beta(y)}{K_{\beta-1}(\zeta)}\frac{K_{\alpha-1}(x)}{K_{\alpha-1}(\zeta)}\left[\frac{2\alpha-3}{2x}\frac{K_\alpha(x)}{K_{\alpha+1}(x)}-1\right]\right\}$$
$$+H(z-s)\frac{x^{\frac{1}{2}}y^{\frac{1}{2}}e^{-\zeta}}{b(\frac{27}{4}-3\alpha^2)}\left\{I_\beta(y)K_\beta(x)\right.$$
$$\left.+I_\alpha(y)K_{\alpha-1}(x)\left[\frac{2\alpha-3}{2y}+\frac{I_{\alpha-1}(y)}{I_\alpha(y)}\right]\left[\frac{2\alpha-3}{2x}\frac{K_\alpha(x)}{K_{\alpha+1}(x)}-1\right]\right\}. \tag{A5}$$

In the above, H denotes the Heaviside function, and

$$\alpha=\sqrt{\frac{1}{4}-\frac{\omega^2\rho}{3\mu_0 b^2}},\quad \beta=\sqrt{\frac{1}{4}-\frac{\omega^2\rho}{\mu_0 b^2}} \tag{A6}$$

$$\zeta=\frac{r}{b},\quad x=\zeta(1+bz),\quad y=\zeta(1+bs) \tag{A7}$$

$$f_1=4\zeta^4+(6\alpha^2-4\alpha\beta+2\beta^2-10\alpha+6\beta+11)\zeta^2+(3\alpha^2\beta^2+6\alpha^2\beta-6\alpha\beta^2-\tfrac{15}{4}\alpha^2-12\alpha\beta+\tfrac{9}{4}\beta^2+\tfrac{15}{2}\alpha+\tfrac{9}{2}\beta-\tfrac{45}{16}) \tag{A8}$$

$$f_2=(4\alpha-6)\zeta^3+(-6\alpha^2+12\alpha-\tfrac{9}{2})\zeta \tag{A9}$$

$$f_3=(4\beta+10)\zeta^3+(6\beta^2+12\beta-\tfrac{15}{2})\zeta \tag{A10}$$

$$f_4=-4\zeta^4-12\zeta^2 \tag{A11}$$

$$f_5=-4\zeta^4-2\zeta^2\beta^2+\tfrac{3}{2}\zeta^2 \tag{A12}$$

$$\Delta(\zeta)=f_1\frac{K_\alpha(\zeta)}{K_{\alpha-1}(\zeta)}\frac{K_\beta(\zeta)}{K_{\beta-1}(\zeta)}+f_2\frac{K_\alpha(\zeta)}{K_{\alpha-1}(\zeta)}+f_3\frac{K_\beta(\zeta)}{K_{\beta-1}(\zeta)}+f_4. \tag{A13}$$

APPENDIX B: EXPRESSIONS FOR $\mathcal{I}_k(m, n, l)$ AND $\mathcal{J}_k(m, l)$

$$\mathcal{I}_k(0,0,0)=\frac{2}{\pi B}F(q) \tag{B1}$$

$$\mathcal{I}_k(0,0,1)=\frac{2d_k}{\pi BD}E(q) \tag{B2}$$

$$\mathcal{I}_k(0,0,2)=\frac{2}{\pi B^3D^3}\{4d_k^2(r^2+a^2+d_k^2)-B^2D^2\}E(q)-\frac{2d_k^2}{\pi B^3D}F(q) \tag{B3}$$

$$\mathcal{I}_k(1,0,0)=-\frac{d_k}{\pi rB}F(q)-\frac{d_k(r-a)}{\pi r(r+a)B}\Pi(q,p)+\frac{1}{r}H(r-a) \tag{B4}$$

$$\mathcal{I}_k(1,0,1) = \frac{1}{\pi rBD}(r^2 - a^2 - d_z^2)E(q) + \frac{1}{\pi rB}F(q) \tag{B5}$$

$$\mathcal{I}_k(1,0,2) = -\frac{d_k}{\pi rB^3D^2}\{4(r^2 + a^2 + d_z^2)(r^2 - a^2 - d_z^2) + 3B^2D\}E(q) - \frac{d_k}{\pi rB^3D}(r^2 - a^2 - d_z^2)F(q) \tag{B6}$$

$$\mathcal{I}_k(0,1,0) = -\frac{d_k}{\pi aB}F(q) + \frac{d_k(r-a)}{\pi a(r+a)B}\Pi(q,p) + \frac{1}{a}H(a-r) \tag{B7}$$

$$\mathcal{I}_k(0,1,1) = \frac{1}{\pi aBD}(a^2 - r^2 - d_z^2)E(q) + \frac{1}{\pi aB}F(q) \tag{B8}$$

$$\mathcal{I}_k(0,1,2) = -\frac{d_k}{\pi aB^3D^2}\{4(r^2 + a^2 - d_z^2)(a^2 - r^2 - d_z^2) + 3B^2D\}E(q) - \frac{d_k}{\pi aB^3D}(a^2 - r^2 - d_z^2)F(q), \tag{B9}$$

$$\mathcal{I}_k(1,1,0) = -\frac{B}{\pi ra}E(q) + \frac{1}{\pi raB}(r^2 + a^2 + d_z^2)F(q) \tag{B10}$$

$$\mathcal{I}_k(1,1,1) = \frac{d_k}{\pi raBD}(r^2 + a^2 - d_z^2)E(q) - \frac{d_k}{\pi raB}F(q) \tag{B11}$$

$$\mathcal{I}_k(1,1,2) = -\frac{1}{\pi raB^3D^2}\{B^2D(r^2 + a^2 + d_z^2) - d_k^2(D^2 + 4raB^2)\}E(q) + \frac{1}{\pi raB^3D}\{B^2D - d_k^2(r^2 + a^2 + d_z^2)\}F(q) \tag{B12}$$

$$\mathcal{I}_k(m,l) = \begin{cases} (-1)^m \dfrac{\partial^m}{\partial d_k^m}\left\{\dfrac{(\sqrt{d_z^2 + r^2} - d_z)^m}{r^m\sqrt{d_z^2 + r^2}}\right\}, & r > 0, \\ \delta_{m0}\dfrac{2^l}{d_z^{l+1}}, & r = 0. \end{cases} \tag{B13}$$

Here $F(q)$, $E(q)$ and $\Pi(q, p)$ are the complete elliptic integrals of the first, second and the third kind, respectively. $H(r-a)$ is the Heaviside step function, and δ_{m0} is the Kronecker delta. Finally,

$$p = \frac{4ra}{(r+a)^2} \tag{B14}$$

$$q = \sqrt{\frac{4ra}{(r+a)^2 + d_z^2}} \tag{B15}$$

$$B = \sqrt{(r+a)^2 + d_z^2} \tag{B16}$$

$$D = (r-a)^2 + d_z^2 \tag{B17}$$

$$d_1 = |z - s| \tag{B18}$$

$$d_2 = z + s. \tag{B19}$$